Coral Reefs
https://doi.org/10.1007/s00338-026-02940-w

RESEARCH

Context-dependent regulation of coral–macroalgae interactions across heterogeneous reef environments

Ibis Tarini López-Jiménez[1] · **Jose Maria Eirin-Lopez**[1]

Received: 24 February 2026 / Accepted: 8 August 2026

Abstract Coral reefs worldwide are declining under multiple anthropogenic stressors, and competitive dynamics between corals and macroalgae are key determinants of reef condition and trajectory. Yet how environmental variation and herbivory jointly shape these interactions remains incompletely resolved. We conducted an 11-month observational field study across four fringing-reef sites on Culebra Island, Puerto Rico, spanning natural gradients in sedimentation, nutrient stoichiometry, seawater temperature, salinity, and *Diadema antillarum* density. Integrated benthic surveys, coral–macroalgae interaction assessments, and exploratory multivariate analyses revealed strong site-level differences in benthic organization. The two sites with higher sedimentation were characterized by lower coral cover and interaction patterns less favorable to coral persistence, whereas the lower-sedimentation sites retained higher coral cover and more mixed benthic assemblages. Macroalgal functional identity significantly influenced competitive outcomes with coral: Filamentous turf algae (FTA) won significantly more contact interactions than either fleshy macroalgae (FA) or coralline algae (CA), while FA was disproportionately represented at coral tissue margins at the two higher-sedimentation sites. Exploratory ordination was broadly consistent with these patterns, identifying sedimentation, *D. antillarum* density, and salinity as the variables most strongly associated with among-site differences in community structure, although the limited four-site observational design precludes strong causal inference. Overall, the results support a context-dependent view of coral–macroalgae interactions in which herbivory appears most likely to contribute to favorable benthic states where local environmental conditions are comparatively less stressful.

Keywords Coral–macroalgae interaction · Phase shift · Herbivory · *Diadema antillarum* · Sedimentation · Caribbean reefs · Marine conservation

Introduction

Coral reefs worldwide face accelerated degradation driven by synergistic anthropogenic stressors including overfishing, eutrophication, sedimentation, and climate change (Hughes et al. 2017a, 2023). A defining characteristic of this degradation involves systematic increases in macroalgae and turf algae (Bellwood et al. 2004; Hughes et al. 2017b; Tebbett et al. 2023), which competitively interact with corals through multiple mechanisms including shading, abrasion, allelopathy, sediment trapping, and microbial pathogenicity (McCook et al. 2001; Rasher and Hay 2010a; Roach et al. 2020). These competitive dynamics intensify in anthropogenically disturbed systems (Barott et al. 2012; Hughes et al. 2017a), where phase shifts from coral to macroalgal dominance occur through interconnected pathways linking herbivore depletion (Bellwood et al. 2006), nutrient enrichment (Littler and Littler 2007; Littler et al. 2009; Lesser 2021), sedimentation (Bessell-Browne et al. 2017; López-Jiménez et al. 2021), and climate change (Hoegh-Guldberg et al. 2017; Hughes et al. 2017a).

Supplementary Information The online version contains supplementary material available at https://doi.org/10.1007/s00338-026-02940-w.

✉ Jose Maria Eirin-Lopez
jeirinlo@fiu.edu

Ibis Tarini López-Jiménez
ilope142@fiu.edu

[1] Institute of Environment, Florida International University, Miami, FL 33181, USA

Published online: 19 August 2026

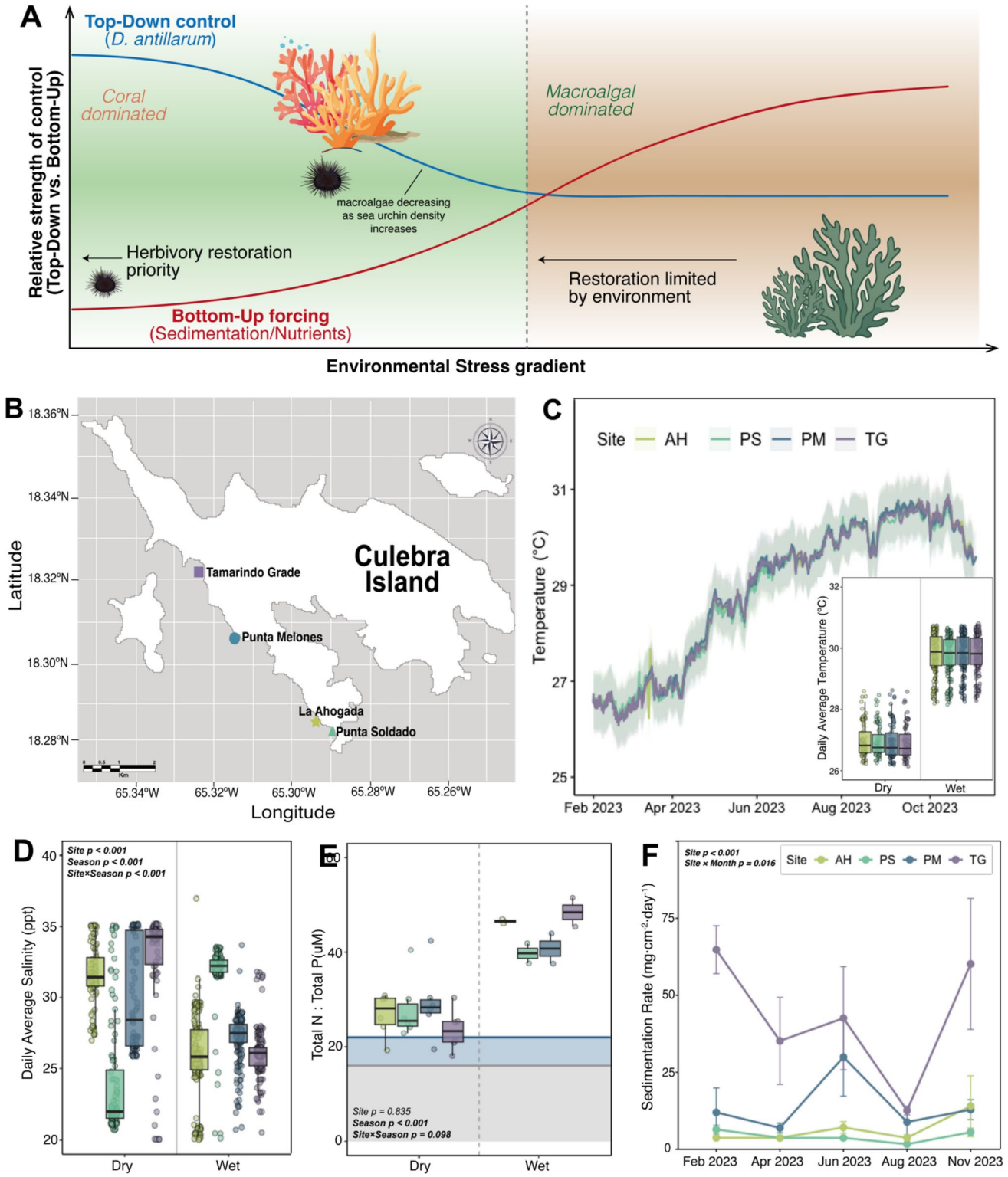

Understanding the mechanisms governing coral–macroalgae competitive outcomes remains critical for predicting ecosystem trajectories and developing effective management interventions. Competitive interactions are highly context dependent, with outcomes varying according to coral morphology (Swierts and Vermeij 2016), macroalgal functional properties (Rasher et al. 2011), and environmental conditions (Vermeij et al. 2010). Critically, macroalgal functional properties—growth form, sediment-trapping capacity, and allelopathic potential—frequently

◂**Fig. 1** Conceptual framework for context-dependent regulation of coral–macroalgae competitive interactions across environmental stress gradients, study site overview, and spatiotemporal dynamics of key environmental parameters across study sites. **(A)** The relative strength of top-down control (*Diadema antillarum*-mediated herbivory; blue) and bottom-up forcing (sedimentation and nutrient loading; red) shifts predictably along an environmental stress gradient. The dashed line represents a hypothetical transition zone, presented here as a working conceptual framework. Under comparatively low environmental stress, top-down control predominates, herbivory suppresses macroalgal proliferation and benthic communities remain coral-dominated (herbivory restoration priority zone; left), whereas under elevated stress, bottom-up forcing overrides herbivory-mediated suppression regardless of urchin density, driving a transition to macroalgal dominance in which restoration outcomes are constrained by the environment (restoration limited by environment zone; right). **B** Study sites on Culebra Island, Puerto Rico, consisting of Tamarindo Grande (TG; N 18.323370º, W 65.328008º), Punta Melones (PM; N 18.307029º, W 65.313742º), La Ahogada (AH; N 18.287880º, W 65.296823º), and Punta Soldado (PS; N 18.280103º, W 65.287875º). **C** Seawater temperature variation across study sites. Solid lines represent daily mean values; shaded envelopes delineate the diurnal thermal range (daily minima and maxima). The inset represents the daily average of seawater temperature (ºC) across sites and seasons. **D** Daily average in salinity across sites and seasons (dry and wet). Box plots display statistical distributions at each site-season combination, while overlaid data points represent individual measurements. **E** Nutrient stoichiometry (total N:P ratios) across study sites and seasons (dry and wet). Reference thresholds include the canonical Redfield ratio (16:1 N, horizontal purple line; (Redfield 1958) and the phosphorus limitation threshold (22:1, horizontal blue line; (Rosset et al. 2017). The gray shaded region demarcates potential nitrogen limitation (ratios ≤ 16:1), while the blue shaded region indicates the transition zone toward phosphorus limitation (ratios between 16:1 and 22:1). **F** Spatial patterns in sedimentation rate ($mg \cdot cm^{-2} \cdot day^{-1}$) by site across period sampling

supersede coral-specific traits in determining interaction outcomes (McCook et al. 2001; Liao et al. 2019).

Turf and fleshy macroalgae represent the principal coral antagonists in contemporary reef systems (Vermeij et al. 2010; Clements et al. 2018), inhibiting coral growth (Jompa and McCook 2003), larval recruitment success (Birrell et al. 2008; Vermeij et al. 2009), and reproductive fecundity (Kuffner et al. 2006; Pozas-Schacre et al. 2024). Turf algae exhibit particularly aggressive competitive strategies through rapid substrate colonization (Cetz-Navarro et al. 2015; Gómez Cubillos et al. 2019), generation of localized hypoxic microenvironments at the coral–macroalgal interface (Wangpraseurt et al. 2012; Haas et al. 2014), physical tissue damage (Thinesh et al. 2019), and enhanced disease susceptibility (Barott and Rohwer 2012; Estrada-Saldívar et al. 2021). The sediment-trapping capacity of turf algae intensifies physiological stress in coral and crustose coralline algae (CCA) populations (Cetz-Navarro et al. 2013) while reducing herbivore grazing efficiency, thereby reinforcing feedbacks that favor algae persistence (Goatley and Bellwood 2013; Tebbett et al. 2018).

Herbivory is a central top-down regulatory mechanism in reef ecosystems, with herbivore biomass reductions precipitating turf and macroalgal proliferation concurrent with coral decline (Hughes et al. 2007; Burkepile and Hay 2010). The long-spined sea urchin *Diadema antillarum* is a keystone grazer in Caribbean systems, exerting a disproportionate influence on benthic-community structure (Lessios 2016). The catastrophic Caribbean-wide *D. antillarum* mass mortality event in 1983–1984 precipitated widespread phase shifts to macroalgal dominance (Lessios 2016). Ongoing restoration efforts suggest that sea urchin population enhancement holds promise for reversing macroalgal dominance under environmentally favorable conditions (Williams 2022), and settlement monitoring provides critical baseline data for evaluating recovery trajectories (Skowronski et al. 2025). However, the herbivore-mediated regulation efficacy appears fundamentally contingent upon environmental context, with nutrient enrichment and sediment loading potentially overwhelming top-down control mechanisms (Burkepile and Hay 2006).

Environmental heterogeneity also shapes reef community reorganization patterns. While acute disturbances such as bleaching events and disease outbreaks can induce rapid regime shifts (Graham et al. 2015), long-term regulation operates through bottom-up control via nutrient availability and sediment loads coupled with top-down herbivore pressure (Burkepile and Hay 2006, 2010; Littler et al. 2009; Shantz et al. 2015). Environmental parameters including seawater temperature, light, salinity, and wave energy exhibit seasonal and spatial variability that modulates macroalgal abundance and assemblages composition (Brown et al. 2019; Harris et al. 2021). Critically, the interaction between environmental stress and herbivory may exhibit patterns consistent with threshold-like dynamics, wherein degraded conditions overwhelm herbivore regulatory capacity and enable transitions to alternative stable states (Hughes 1994; Bellwood et al. 2006).

Despite extensive conceptual work, important gaps remain in understanding how environmental gradients and herbivory jointly shape coral–macroalgae competitive outcomes in contemporary Caribbean reefs. In particular, the extent to which recovering *Diadema antillarum* populations can influence benthic organization across contrasting environmental settings remains unresolved. To address this gap, we conducted an integrated 11-month observational field study across four fringing-reef sites on Culebra Island, Puerto Rico, spanning natural gradients in sedimentation, nutrient stoichiometry, salinity, seawater temperature, and *D. antillarum* density. Because Culebra lacks permanent rivers and continuous freshwater inputs, we interpret salinity primarily as a hydrographic indicator that covaries with rainfall-driven runoff and local hydrodynamic exchange rather than as an independent causal

driver. We hypothesized that coral–macroalgae interaction outcomes would vary with environmental context, such that sites experiencing higher sedimentation and associated environmental stress would show lower coral cover and interaction patterns less favorable to coral persistence, whereas the influence of *D. antillarum* would be more evident at sites under comparatively lower environmental stress (Fig. 1A).

Materials and methods

Study site characterization and environmental monitoring

This investigation was conducted across four shallow-water fringing-reef sites (2–7 m depth) on Culebra Island, Puerto Rico, during an 11-month period from February through December 2023. Although our environmental monitoring encompassed a single annual cycle (2023), the continuous records and sampling of environmental data (*i.e.,* seawater temperature, salinity, sedimentation rate, and nutrients input) and the three strategically timed benthic surveys capture the principal seasonal contrasts at each site. Interannual variability associated with ENSO forcing, hurricane disturbance, or long-term anthropogenic change cannot be assessed from the present dataset and represents an important direction for future monitoring efforts. The selected sites (Tamarindo Grande (TG), Punta Melones (PM), La Ahogada (AH), and Punta Soldado (PS)) were chosen to span natural gradients in nutrient availability, sedimentation, and herbivore abundance (Fig. 1B). Environmental parameters were monitored continuously over the eleven months. Seawater temperature and salinity were recorded every hour using Onset HOBO Pendant MX Temperature Data loggers and HOBO Salt-Water Conductivity/Salinity Data Loggers, respectively. Sedimentation was quantified using replicate (n = 4 per site) PVC tubing sediment traps (45 cm tall, 6.4 cm aperture diameter), retrieved every six weeks. Sedimentation rate ($mg \cdot cm^{-2} \cdot day^{-1}$) was calculated by dividing the weight of dried sediment by the size of the trap opening and deployment duration (Otaño-Cruz et al. 2017). Nutrient levels (total nitrogen and total phosphorus) were assessed every six weeks, concurrent with sediment traps retrieval, using the brown macroalgae *Dictyota* sp. as a bioindicator following established protocols validated for Caribbean waters (Todd et al. 2009). At each sampling interval, three replicate samples of *Dictyota* sp. were collected haphazardly at each site (n = 3 samples per site per interval; 96 samples in total), immediately frozen, and analyzed at the CAChE-Nutrient Analysis Core Facility at FIU.

Benthic cover assessment and coral–macroalgae interaction assessment

Field sampling was conducted under Puerto Rico Natural Resources Department permit 2023-IC-008. Benthic composition was quantified using standardized photoquadrat surveys (Preskitt et al. 2004) conducted at three time points (March, July, November 2023) spanning dry and wet seasons. At each site, eight 20 m^2 belt transects (10 m × 2 m) were established parallel to the coastline across the 2–7 m depth range, with transects separated by 10–20 m to promote spatial independence while maintaining comparable reef habitat. Sampling quadrats (0.5 × 0.5 m; Fig. S1A) were positioned at one-meter intervals along each transect, yielding = 288 quadrats per site (8 transects × 12 quadrats × 3 sampling periods). Digital images were captured using an Olympus TG-6 camera (12-megapixel resolution) mounted on a standardized tripod frame and analyzed with Coral Point Count with Excel extensions (CPCe) software, using 50 randomly distributed points per quadrant (Preskitt et al. 2004; Kohler and Gill 2006). Benthic organisms were categorized into broad taxonomic and functional groups to ensure consistency across the photographic dataset: hard corals (Branching *Porites* spp., *Porites astreoides*, encrusting, and massive forms), benthic algae (filamentous turf algae (FTA), fleshy macroalgae (FA, including *Dictyota* sp., *Lobophora* spp., *Halimeda* spp., and other foliose taxa), and coralline algae (CA, including crustose coralline and other calcareous taxa)), and other benthic organisms (sponges, soft corals). This functional-group classification, while consistent with standard photoquadrat methodology (Preskitt et al. 2004; Kohler and Gill 2006), operates at a resolution that precludes species-level attribution of among-site differences in benthic composition. Non-biological substrates were classified as sand, pavement, rock, rubble, and dead coral.

Coral–macroalgae interactions were quantified using complementary line-intercept methods (Barott et al. 2009). During each sampling period, we surveyed all coral colonies exhibiting visible macroalgal contact along established transects, yielding 606 unique coral–macroalgae contact records across all sites and sampling periods. For each interaction, we recorded coral morphology (branching, massive, encrusting), macroalgal functional group (CA, FTA, FA), and competitive outcome. Interaction outcomes were classified following established criteria (Barott et al. 2012) as: (i) coral win, when coral tissue advanced across the interface and/or the algal thallus showed loss at the contact margin or causing visible algal tissue damage; (ii) macroalgal win, when coral tissue edges displayed tissue necrosis, discoloration, bleaching,

or clear macroalgal overgrowth; and (iii) neutral interaction, showing no apparent competitive advantage, with stable boundary and no visible tissue damage on either organism (Figs. S1B-C). These categories describe the interaction state observed at the time of sampling and are expected to vary seasonally as colony growth rates and physiological condition change. Outcome determination was based on visual assessment of tissue condition and growth patterns at interaction boundaries, supplemented by photographic documentation for quality control and independent verification of ambiguous cases.

To evaluate whether macroalgal functional groups were proportionally overrepresented at coral tissue edges relative to their background abundance in the benthos, we computed a contact enrichment index as the difference between each functional group's proportional representation among all coral–macroalgal contact records and its proportional cover in concurrent photoquadrat surveys at the same site. Positive values indicate enrichment at coral borders relative to background; negative values indicate underrepresentation. Contact proportions along coral margins were measured using complementary video recordings and ImageJ software (Abràmoff et al. 2004). Contact proportion was calculated by dividing macroalgal contact length by total coral perimeter. This metric provides size-independent quantification of interaction intensity, enabling comparisons across coral colony sizes and morphologies. Corals were grouped by focal taxa/morphology (Branching *Porites* spp., *Porites astreoides*, and all other hard corals, which were further classified as encrusting (substrate-adhering, without vertical growth) or massive (isometric growth) forms).

Sea Urchin population assessment

Diadema antillarum population density was quantified using belt transects (10 m × 2 m; 20 m^2 area) conducted at six-week intervals throughout the study period. Eight replicate transects were surveyed at each site during each sampling period, positioned parallel to and interspersed with benthic photoquadrat transects to ensure spatial correspondence between herbivore abundance and benthic-community data. Surveys were conducted during daylight hours (0900–1500 h) when sea urchins occupy diurnal refugia in crevices and under coral colonies, enabling systematic detection through visual search of cryptic microhabitats to maximize detection probability. Surveyed individuals were classified into three size classes based on the test diameter: small (< 4 cm), medium (4–6 cm), and large (> 6 cm) for population size structure (Mercado-Molina et al. 2015; Rodríguez-Barreras et al. 2023). Density (ind·m^{-2}) was calculated for each transect and averaged across replicates to estimate site-level abundance.

Statistical analyses

All statistics were conducted in R (version 4.0.3; R Core Team, 2024) using the *car* package (Fox and Weisberg 2018). Given the limited study sites (n = 4), we emphasize effect sizes and confidence intervals alongside p-values. Data screening included visual and test-based normality checks (histograms, Q-Q plots, Shapiro–Wilk), and homogeneity tests (Levene). When parametric assumptions were violated ($p < 0.05$) and when standard transformations (log, square root, arcsine square root for proportional data) failed to satisfy parametric assumptions—particularly in variables exhibiting zero-inflated, right-skewed distributions—we employed nonparametric alternatives or robust variance estimators (Welch corrections for ANOVA), which relax the homoscedasticity assumption without imposing potentially unrealistic distributional constraints on compositional data. Seasons were classified following Caribbean conventions: dry season (December–April) and wet season (May–November). All primary hypotheses employed $\alpha = 0.05$. Environmental variables (total N, total P, N:P ratio, sedimentation, water temperature, and salinity) were modeled using generalized linear models (GLMs), with site, season, and their interaction as fixed factors. Distribution families (Gaussian, Gamma, or inverse Gaussian) were selected based on Akaike Information Criterion (AIC); significant effects were followed by pairwise comparisons using estimated marginal means (*emmeans* package) with Tukey adjustments.

Coral and macroalgal cover were analyzed using linear mixed-effects models with site, season, and their interaction as fixed effects, and transect nested within site as a random intercept to account for repeated sampling. Model assumptions were evaluated using residual diagnostics. Because site-only comparisons of benthic cover also violated parametric assumptions, we additionally used Kruskal–Wallis tests followed by Dunn's post hoc comparisons with Bonferroni correction to provide nonparametric confirmation of site-level differences. Effect sizes for these nonparametric comparisons were summarized using rank-based eta-squared (η^2) estimates. Multivariate community structure was assessed via PERMANOVA (*adonis2* function, *vegan* package) with 999 permutations. Community composition patterns were visualized through non-metric multidimensional scaling (nMDS) ordination using Bray–Curtis's dissimilarity matrices, with environmental vectors fitted post hoc using the *envfit* function.

Coral–macroalgae outcomes were analyzed using generalized linear mixed models (GLMMs) with binomial error distributions and coral colony identity entered as a random intercept, accounting for the non-independence of repeated observations from the same colony across sampling periods or multiple contact records along its perimeter. Fixed effects comprised site, macroalgal functional

group, and coral morphological category. Type III Wald χ^2 tests evaluated significance, with pairwise comparisons via estimated marginal means using Tukey corrections. Effect sizes were expressed as odds ratios with 95% confidence intervals. Additionally, χ^2 tests of outcome distributions were based on contingency tables comparing three macroalgal functional groups across three competitive outcome categories (*i.e.,* df = (3 functional groups-1) × (3 outcome categories-1) = 4).

Diadema antillarum density was analyzed using two-way ANOVA with site and season as fixed factors. All belt-transect surveys conducted throughout the 11-month study period were included in the analysis, with season as a covariate. The site-level summary statistics (mean density ± SE per site) were computed across all sampling events. Size-class distributions were evaluated via Kruskal–Wallis tests with Dunn's pairwise post hoc comparisons. To evaluate coral–macroalgal relationships under non-normality and zero-inflated conditions, coral cover and macroalgae cover were log(x + 1) transformed prior to analysis. Model selection using AIC confirmed that log-linear models provided a consistently better fit relative to untransformed linear models. Site-specific Spearman rank correlations were first used to evaluate monotonic associations without assuming normality. Complementary generalized linear models with a Tweedie error distribution were fitted to the same benthic cover data, as this distribution family accommodates semicontinuous, zero-inflated responses with positive continuous components, making it well suited to benthic cover datasets of this type. Model results were interpreted conservatively, with emphasis on effect size, direction, and consistency across methods rather than on marginal trends alone.

When significant site × season interactions were detected, between-group comparisons in the main text were based on means averaged across seasons but interpreted in the context of those interactions. Interaction terms are reported explicitly, and figures provide the seasonal detail that site-level means alone do not capture. To assess environmental-biological interaction, we employed: (1) binomial logistic regression to evaluate environmental predictors of competitive outcomes (McFadden's pseudo-R^2); (2) redundancy analysis (RDA) partitioning community variation among environmental factors, coral cover, macroalgal cover, and *D. antillarum* density with forward selection and permutation tests (999 permutations); and (3) correlation analyses (Spearman or Pearson) to quantify relationships among variables. Because the study included only four sites, the RDA and site-level correlations were interpreted descriptively rather than inferentially. Accordingly, emphasis was placed on identifying broad ecological patterns and context-dependent associations rather than establishing definitive causal relationships.

Results

Environmental conditions across spatial and temporal gradients

Environmental parameters varied strongly across sites (Fig. 1C-F). Seawater temperature (daily mean, derived from hourly logger recordings) varied significantly among sites and seasons, with significant site × season interaction (ANOVA, site $p < 0.001$, season $p < 0.001$, site × season $p = 0.037$; Fig. 1C). Tamarindo Grande (TG) experienced the warmest water temperatures (mean ± SE: 28.9 ± 0.2 °C) and the greatest daily amplitude, while La Ahogada (AH) was slightly cooler on average (28.3 ± 0.3 °C) and more thermally stable (Fig. S2A). Similarly, salinity differed significantly across sites with significant site × season interactions (ANOVA, site $p < 0.001$, season $p < 0.001$, site × season $p < 0.001$; Fig. 1D), with AH and TG consistently exhibiting lower values (34.8 ± 0.1 and 35.1 ± 0.1 ppt, respectively), than Punta Melones (PM) and Punta Soldado (PS) (36.2 ± 0.1 and 36.4 ± 0.1 ppt; $p < 0.001$ for all pairwise comparisons; Fig. S2B). The significant site × season interaction showed that this among-site ranking was not stable across seasons: At AH and TG, salinity was higher in the dry season and lower in the wet season, whereas this seasonal pattern was reversed at PS (lower in the dry season, higher in the wet season) and comparatively muted at PM (Fig. 1D). Pairwise contrasts among site-by-season combinations (estimated marginal means) supported the magnitude and significance of these within-site seasonal differences (Table S1A).

Despite spatial homogeneity in total nitrogen and phosphorus concentrations (N, $p = 0.940$; P, $p = 0.526$; Figs. S2C–D), N:P ratios varied significantly between seasons (ANOVA, $p < 0.001$), averaging 18.4 ± 2.1 during the dry season and 12.8 ± 1.8 during the wet season (Figs. S2E-F). Although N:P ratios were homogeneous across sites ($p = 0.835$; Fig. S2G), individual sites occasionally exhibited values exceeding the phosphorus limitation threshold (22:1), particularly during dry periods (Fig. 1E); however, the site × season interactions were not significant for total N ($p = 0.461$), total P ($p = 0.797$), or N:P ($p = 0.098$; Fig. 1E). Sedimentation showed a significant site effect (ANOVA, $p < 0.001$) with no significant seasonal main effect ($p = 0.349$) and no significant site × season interaction ($p = 0.162$). Sites TG and PM had significantly elevated rates (41.9 ± 15.7 and 14.4 ± 12.4 mg·cm^{-2}·day^{-1}, respectively) relative to PS and AH (4.2 ± 2.3 and 6.2 ± 7.2 mg·cm^{-2}·day^{-1}, respectively; Fig. 1F, Fig. S2H). Despite the absence of significant interaction, Fig. 1F illustrates that temporal variability differed among sites: AH and PS maintained consistently low deposition throughout the monitoring period, whereas TG exhibited pronounced temporal variability consistent with episodic depositional events during wet-season periods

(Fig. 1F). Together, these observations place the four sites along a descriptive gradient from low- to high-stress conditions: AH as a low-stress reference site (moderate temperature, high salinity, low sedimentation, highest coral cover, effective urchin herbivory); PS as a transitional low-moderate stress site with distinctive herbivore dynamics; PM as a moderate-high-stress site; and TG as the highest-stress site (warmest temperatures, lowest salinity, greatest sedimentation, macroalgal-dominated benthos).

Benthic-community structure and coral–macroalgae interaction dynamics

Benthic-community composition showed significant variability across sites and seasons (PERMANOVA, sites $p = 0.001$, seasons $p = 0.001$, site × season $p < 0.01$; Fig. 2A). Hard coral cover differed among sites and seasons, with a significant site × season interaction (LMM: site $p < 0.001$, $\eta^2 = 0.224$; season $p < 0.001$ $\eta^2 = 0.016$; site × season $p < 0.01$; Fig. 2B). Coral cover was highest at AH (13.4 ± 1.1%, mean ± SE) and PS (6.0 ± 0.8%), and lowest at PM (3.5 ± 0.7%) and TG (2.8 ± 0.5%). Pairwise contrasts showed that coral cover at AH and PS significantly exceeded both PM and TG ($p < 0.001$; Table S1B). The significant site × season interaction ($p < 0.01$) showed that between-site differences in coral cover were not seasonally uniform: AH exhibited the greatest dry-to-wet amplitude while differences at PM and TG were comparatively attenuated (Fig. 2B). A nonparametric Kruskal–Wallis' test supported significant site-level differences in coral cover ($\chi^2 = 86.07$, $p < 0.001$), corroborating the LMM results.

Macroalgal cover similarly differed among sites (Kruskal–Wallis: $\chi^2 = 85.5$, $p < 0.001$), with PS displaying highest values (18.5 ± 1.0%, mean ± SE), followed by AH (12.6 ± 1.1%), and lower cover at PM (8.4 ± 0.8%) and TG (7.9 ± 0.8%; Fig. 2C). Statistical models indicated substantial site effects (LMM, $p < 0.001$, $\eta^2 = 0.11$), significant seasonal variation ($p = 0.015$), and significant site × season interaction ($p = 0.041$). Pairwise contrasts showed significant dry-to-wet differences in macroalgal cover at AH and PS (both $p < 0.05$; Table S1C), but not at PM or TG (both $p > 0.05$). Among sites, PS exceeded AH ($p < 0.001$), PM ($p = 0.002$), and TG ($p < 0.001$), whereas AH exceeded TG ($p = 0.039$) but did not differ from PM ($p = 0.258$); PM and TG were similar ($p = 0.833$). Functional-group composition varied across sites (ANOVA, $p < 0.001$). Coralline algae (CA) maintained low abundance across all sites (< 0.4% cover); fleshy macroalgae (FA) dominated at PS (9.7% cover), while filamentous turf algae (FTA) exhibited relatively uniform distribution (5.3–9.8% cover). Coral taxonomic composition also displayed site-specific patterns (ANOVA, $p < 0.001$), with branching *Porites* spp. more abundant at AH (4.8% cover), and *P. astreoides* showing more consistent distribution (1.1–4.8% cover).

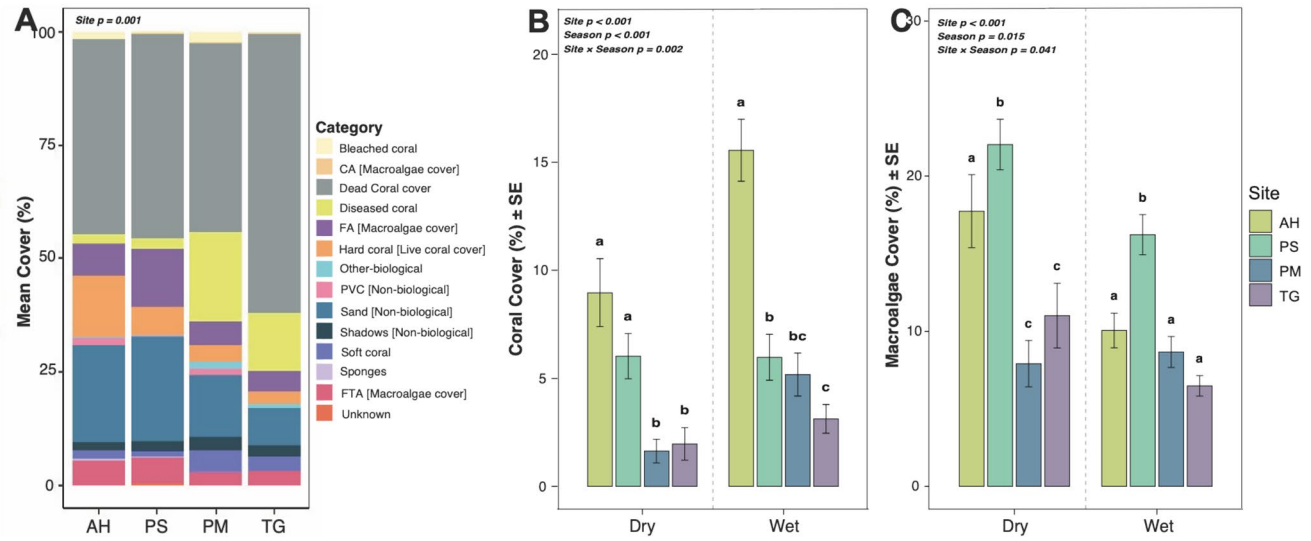

Fig. 2 Benthic-community composition and cover dynamics across study sites. (A) Mean percentage cover of benthic functional groups and constituent taxa across the four study sites (La Ahogada (AH), Punta Soldado (PS), Punta Melones (PM), and Tamarindo Grande (TG)) averaged across the three survey periods (March, July, and November 2023, N = 8 transects per site). Stacked bars represent the proportional contribution of each taxon to total benthic cover; taxa are grouped by functional category, denoted by bracketed annotations in the legend: hard coral [Branching *Porites* spp., *Porites astreoides*, encrusting corals, and massive corals]; coralline algae (CA) [crustose coralline algae and other calcareous taxa]; filamentous turf algae (FTA); fleshy macroalgae (FA) [Dictyota spp., Lobophora spp., Halimeda spp., and other foliose taxa]; and Non-biological substrate [sand, pavement, rock, and rubble]; **(B)** percentage of live coral cover across sites and seasons (dry and wet), and **C** percentage of macroalgae cover across sites and seasons (dry and wet). Bars represent means, and error bars indicate ± 95% confidence intervals. Different lowercase letters denote significant differences among sites

Coral–Macroalgae competitive outcomes are mediated by functional identity and environmental context.

To evaluate whether macroalgal functional groups were proportionally over- or underrepresented at coral tissue margins relative to their background benthic abundance, we computed a contact enrichment index for each site (see Sect. "Benthic cover assessment and coral–macroalgae interaction assessment"; Fig. 3A). Analysis revealed significantly non-random interaction patterns that varied among sites: CA was significantly more abundant at coral borders at AH and TG (t-tests, $p < 0.05$), while FA was significantly overrepresented at PM and TG (t-tests, $p < 0.05$), and FTA showed the most consistent abundance across multiple sites with higher abundance at PS ($t = 3.9$, $p < 0.001$) and PM ($t = 2.9$, $p = 0.001$). These patterns showed that the macroalgal assemblage encountered at coral edges reflects both background community composition and potentially functional-group-specific competitive dynamics that are not reducible to benthic abundance alone.

Analyses of 606 coral–macroalgae contact records using generalized linear mixed models (coral identity as a random intercept) showed significant site-effects variation in the probability of coral "wins" (Type III Wald χ^2, Site $p = 0.028$; $\eta^2 = 0.22$). Coral "win" probability was highest at AH (39.0%), decreasing progressively through PS (33.1%), PM (23.2%), and TG (11.1%; Fig. 3B, S3A). Pairwise comparisons supported that AH had significantly higher coral-win probabilities than PM ($\chi^2 = 5.25$, $p = 0.028$) and PS ($\chi^2 = 4.98$, $p = 0.031$). Across all sites, macroalgal "wins" exceeded coral wins overall, particularly in interactions with FTA and FA functional groups (Fig. 3C). Neutral and coral-win outcomes were most frequent at AH and PS, whereas macroalgal-win outcomes predominated at PM and TG (Kruskal–Wallis tests, CA $p < 0.048$, FA $p = 0.031$; Fig. 3B-C).

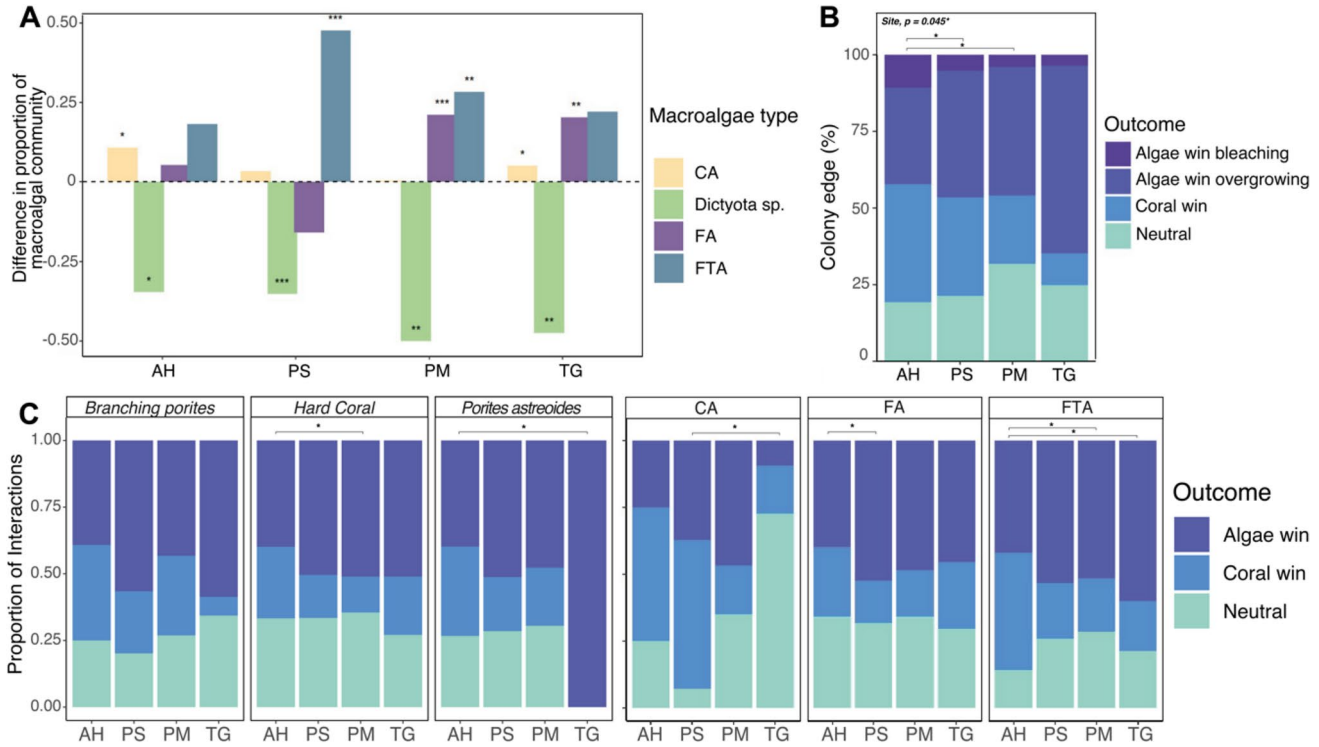

Fig. 3 Coral–macroalgae outcomes and interactions assessments. **A** Contact enrichment index for the three macroalgal functional groups at each study site. The index was calculated as the difference between each group's proportion among all recorded coral–macroalgal contact events and its proportional cover in concurrent benthic photoquadrat surveys at the same site and sampling period. Positive values indicate overrepresentation at coral tissue margins relative to background abundance, and negative values indicate underrepresentation. Statistical significance of departures from zero was assessed using one-sample t-tests. Asterisks denote statistical significance (*$p < 0.05$, **$p < 0.01$, ***$p < 0.001$). AH: La Ahogada; PS: Punta Soldado; PM: Punta Melones; TG: Tamarindo Grande. **(B)** Distribution of the defined competition outcome categories across sites, categorized as algal win via bleaching, algal win via overgrowing, coral win, or neutral. **(C)** Proportional distribution of competitive outcomes (algal win, coral win, neutral) partitioned by coral morphological category (branching *Porites* spp., hard coral, *Porites astreoides*; left panels) and macroalgal functional identity group (coralline algae, CA; fleshy algae, FA; filamentous turf algae, FTA; right panels) across sites, illustrating treatment-specific response patterns. Asterisks above bars denote significant pairwise contrasts (*$p < 0.05$) derived from chi-square tests; bracket annotations indicate specific site comparisons within each functional group. Bonferroni-adjusted threshold for six pairwise comparisons is $p < 0.0083$

Competitive outcomes distributions differ significantly among macroalgal functional identity groups (χ^2 (4) = 15.35, $p = 0.004$; Fig. 3C), driven primarily by FTA dominating contact interfaces relative to both CA ($p < 0.01$) and FA ($p < 0.01$), while CA and FA did not differ from one another ($p = 0.237$; Figs. S3B-E). Competitive outcomes between corals and FTA differed significantly at TG and PM (both $p < 0.001$; Fig. S3D) but were statistically indistinguishable at PS and AH (all $p > 0.05$). In contrast, FA-mediated outcomes showed comparatively little site-level variation (global $p = 0.196$), with only a borderline pairwise contrast between AH and PS ($p = 0.042$). Coral morphological identity did not significantly influence competitive vulnerability across any functional-group category (Branching *Porites* spp.: $p = 0.547$; Hard Coral: $p = 0.051$; *P. astreoides*: $p = 0.191$; Figs. 3C, S3F). However, descriptive inspection of outcomes distributions stratified by coral morphology and macroalgal functional group showed that branching *Porites* spp. had a higher proportion of coral wins in interactions involving FA relative to encrusting and massive morphologies (Figure S3F).

Diadema antillarum population structure shows demographic variation and environmental constraints

A total of 390 live *D. antillarum* individuals were recorded across sites and sampling periods. *Diadema antillarum* densities differed significantly across sites (ANOVA, $p < 0.001$) but not across seasons ($p = 0.792$), with the site × season interaction not reaching statistical significance ($p = 0.851$). Mean sea urchin density was highest at AH (0.17 ± 0.13 ind·m^{-2}) and lowest at PS (0.05 ± 0.10 ind·m^{-2}), with intermediate values at PM and TG (PM: 0.12 ± 0.11, TG: 0.08 ± 0.09; Fig. 4A). Post hoc comparisons showed AH densities significantly exceeded all other sites ($p < 0.01$), while PS had significantly lower density than AH and PM ($p < 0.001$ and $p = 0.023$, respectively). Mean sea urchin size also varied significantly across sites ($p < 0.001$) and season ($p = 0.025$), with individuals at AH significantly greater than at PS and TG ($p < 0.001$). At AH and PM populations contained higher proportions of medium (40–60 mm) and large (> 60 mm) individuals (Fig. 4B), whereas PS and TG populations were dominated by small individuals (< 40 mm).

Environmental-Biological integration reveals context-dependent regulatory mechanisms

Redundancy analysis (RDA) was used as an exploratory multivariate framework relating environmental predictors (sedimentation, salinity, temperature, N:P ratio, and *D. antillarum* density) to benthic-community composition (Fig. 5A). The model collectively explained 55.7% of community variation, although the global model was not statistically significant ($p = 0.948$; Fig. 5A). Forward selection

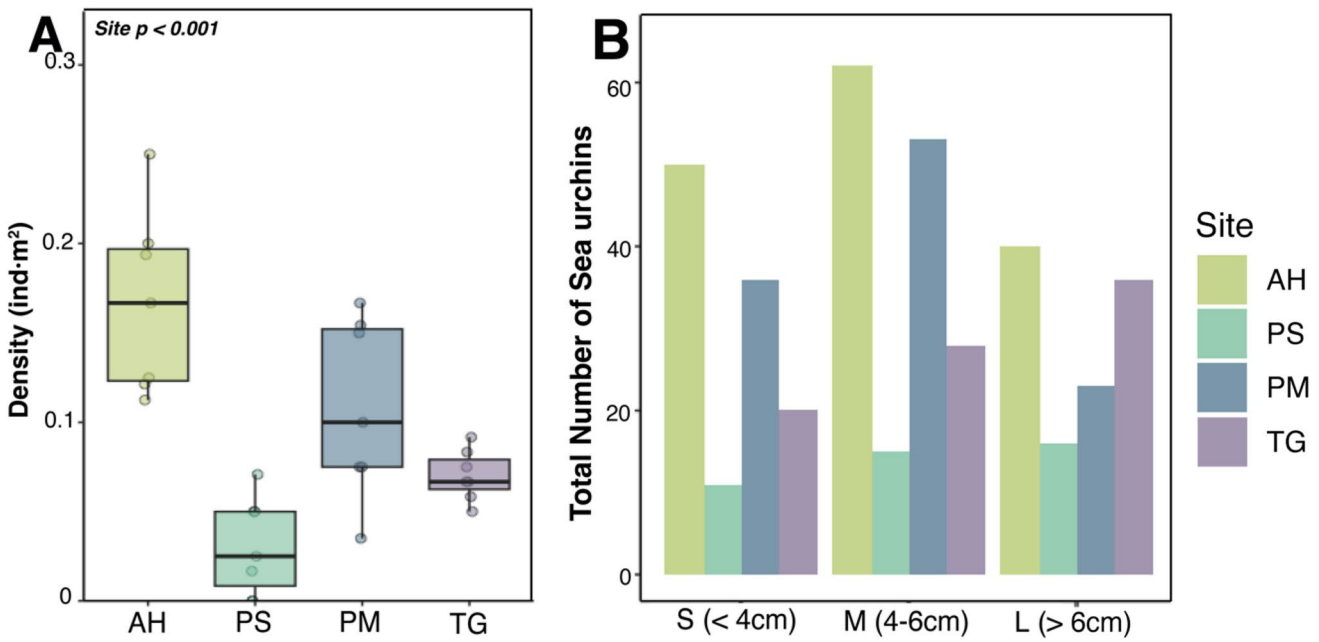

Fig. 4 Population structure and demographic characteristics of *D. antillarum* assemblages. (A) Spatial variation in *Diadema antillarum* density (ind·m^{-2}) by site across all sampling events, derived from standardized belt transects and presented as means ± 95% confidence intervals. **B** Size-frequency distributions by site, classified into small (< 40 mm), medium (40–60 mm), and large (> 60 mm) test-diameter classes. Bars represent means; error bars represent ± 95% CI. AH: La Ahogada, PS: Punta Soldado, PM: Punta Melones, TG: Tamarindo Grande

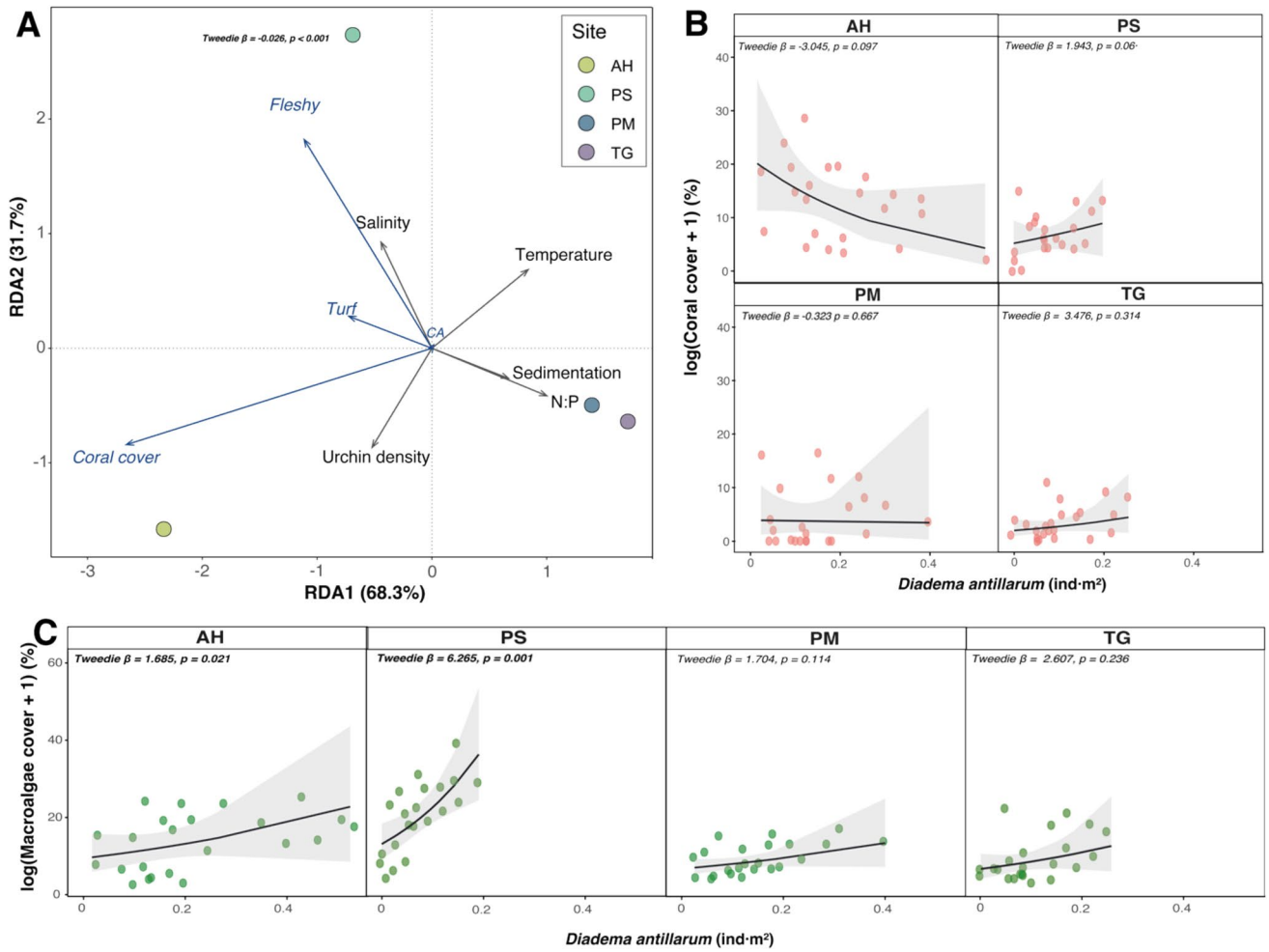

Fig. 5 Benthic cover relationships across environmental gradients and site-specific associations between coral cover, macroalgal cover, and *Diadema antillarum* density at the four study sites. **A** Constrained redundancy analysis (RDA) relating benthic-community composition to measured abiotic predictors (sedimentation, salinity, water temperature, N:P ratio, and *D. antillarum* density. Ordination axes are RDA1 (68.3% of constrained variance) and RDA2 (31.7%); site observations are shown as colored symbols: La Ahogada (AH), Punta Soldado (PS), Punta Melones (PM), and Tamarindo Grande (TG). Arrows indicate the direction and relative strength of associations between environmental predictors and the ordination axes. Gray arrows represent environmental explanatory variables, and blue arrows indicate benthic response variables. **B** Site-specific relationships between *D. antillarum* density (ind·m^{-2}) and log(x + 1)-transformed coral cover (%). **C** Site-specific relationships between *D. antillarum* density (ind·m^{-2}) and log(x + 1)-transformed macroalgal cover. In panels B–C, points are colored by site: La Ahogada (AH), Punta Soldado (PS), Punta Melones (PM), and Tamarindo Grande (TG). Fits are shown with 95% confidence intervals. Solid lines represent Tweedie generalized linear model fits with shaded 95% confidence bands; site-specific Tweedie coefficients (β) and p-values are reported within each panel (see also Table S2)

and permutation testing nonetheless identified sedimentation (17.7%), *D. antillarum* density (16.9%), and salinity (16.4%) as primary contributors to constrained variance, while N:P ratio and temperature contributed minimally (3.8% and 0.9%, respectively). Because the global RDA fit was non-significant, the ordination is interpreted descriptively rather than as formal axis-level inference; Fig. 5A is therefore presented as a visual summary of multivariate distributional tendencies across sites rather than a validated statistical model.

To clarify the directionality of these associations, we constructed a coral–macroalgal interaction index for each sampling unit, defined as coral cover minus macroalgal cover (%); positive values indicate conditions more favorable to coral persistence, and negative values indicate conditions more favorable to macroalgal (Figure S4). Univariate linear regression analyses of this index against each environmental predictor identified three significant relationships: salinity (β = -7.7, $p = 0.016$; Fig. S4A) and sedimentation rate (β = -81.2, $p < 0.029$; Fig. S4B) were negatively associated with interaction index, and *D. antillarum* density was positively related (β = 659.7, $p = 0.026$; Fig. S4C). The N:P ratio showed a negative but only marginally non-significant association (β = -2.9, $p = 0.053$; Fig. S4D). Within the relatively

narrow thermal range observed among sites, temperature (β = 27.5, *p = 0.063*; Fig. S4E) was not significantly related to the interaction index. Across the observed environmental range, sedimentation explained the greatest predicted change in the interaction index (Fig. 5A, S4B).

A complementary binomial logistic regression modeled the probability of a macroalgal, rather than coral, win at the level of individual coral–macroalgal interactions (606 interaction observations nested within four sites) as a function of the same environmental predictors. Among these *D. antillarum* density was the only significant predictor (β = -3.06, *p = 0.0008*): Higher urchin density was associated with greater probability of coral dominance during coral–macroalgal encounters; a finding now directly corroborated by the significant positive relationship between urchin density and the site-level interaction index reported above (Fig. S4C). This convergence across two independent analytical scales (i.e., individual contact outcomes and whole-community cover balance) provides additional support that *D. antillarum* density is consistently associated with coral competitive standing across analytical scales. However, given the strong spatial covariance between herbivore density and other site-level characteristics inherent to this four-site design, we interpreted the logistic-regression result cautiously, as consistent with, rather than proof of, an independent, context-independent herbivory effect.

To resolve whether this between-site covariance reflected a direct, within-site dose–response relationship, we fitted site-specific Tweedie generalized linear models relating transect-level *D. antillarum* density to coral cover (Fig. 5B) and macroalgal cover (Fig. 5C) independently, accommodating the zero-inflated structure of both response variables (Table S2). Coral cover showed no statistically significant relationship with urchin density at any site (AH: β = −3.045, *p = 0.097*; PS: β = 1.943, *p = 0.060*; PM: β = −0.323, *p = 0.667*; TG: β = 3.476, *p = 0.314*). By contrast, macroalgal cover was significantly and positively associated with urchin density at two of the four sites (AH: β = 1.685, *p = 0.021*; PS: β = 6.265, *p = 0.001*), with comparable, non-significant positive associations at the remaining two sites (PM: β = 1.704, *p = 0.114*; TG: β = 2.607, *p = 0.236*). In addition, the within-site *D. antillarum* density influencing the coral–macroalgae relationships were divergent across sites (Fig.S5). At AH transects with higher *D. antillarum* density exhibited a significant negative coral–macroalgae association (Tweedie β = −0.693, *p < 0.001;* Fig. S5A). At PS, a statistically significant positive relationship of comparable magnitude (β = 2.856, *p = 0.002;* Fig. S5B), the inverse of the pattern observed at AH. At PM and TG, no coherent relationship was apparent (PM: β = 0.757, *p = 0.084;* TG: β = -0.940, *p = 0.274;* Figs. S5C-D). These contrasts are consistent with a context-dependent association between *D. antillarum* and benthic composition; but the present observational dataset does not allow discrimination between herbivore effects and shared environmental drivers. Accordingly, the observed coral–macroalgae relationships should be interpreted as patterns of covariation rather than evidence of direct causation.

Integrating these site-level results with the broader environmental gradient described in Sect. "Environmental conditions across spatial and temporal gradients", the two sites with comparatively lower average sedimentation rates (AH and PS) retained higher coral cover and more mixed benthic assemblages at the site level (Figs. 1F, 2B), whereas the two sites with higher average sedimentation rates (TG and PM) were characterized by persistently low coral cover and interaction patterns less favorable to coral persistence (Figs. 1F, 2B–C, 3B–C).

Discussion

Environmental drivers of Coral–Macroalgae interaction

Our integrated field assessment across natural environmental gradients was broadly consistent with the idea that coral–macroalgae competitive outcomes emerge from the combined influence of multiple co-occurring stressors rather than from any single dominant driver. Across the four study sites, variation in sedimentation, salinity, nutrient stoichiometry, temperature, and *D. antillarum* density coincided with clear differences in coral cover, macroalgal representation at coral margins, and competitive outcome distributions. Exploratory multivariate analysis was broadly consistent with these site-level patterns, although the non-significant global RDA fit (*p = 0.948*) indicates that the ordination should be interpreted descriptively rather than as evidence for formal partitioning of causal effects.

Sites experiencing elevated sediment deposition (TG, PM) consistently exhibited reduced coral cover and extensive coral–macroalgae contact zones, identifying sedimentation as a primary correlate of community degradation consistent with established coral physiology paradigms (Fabricius 2005; Goatley and Bellwood 2013). Nevertheless, the observed covariation between sedimentation rate and coral–macroalgae interaction index (β = -81.2, *p = 0.029*; Fig. S4B) is compatible with the interpretation that chronic sediment stress can alter competitive balance at the coral–macroalgal interface, potentially through impaired light availability, sediment abrasion on coral tissue, and reduced herbivore grazing efficiency (Fabricius 2005; Goatley and Bellwood 2013; Gowan et al. 2014; Brown et al. 2018; Liao et al. 2019). N:P ratio varied significantly between seasons but not among sites (ANOVA, *p < 0.001*; Figs. 1E, S2G), suggesting that nutrient stoichiometry

provided a temporally dynamic backdrop rather than a strong spatial predictor of benthic organization in this study. Notably, the two higher-sedimentation sites tended to show greater temporal variability in N:P, consistent with the possibility that nutrient dynamics and sedimentation covary through episodic runoff inputs. Because N:P ratios were spatially homogeneous and site-level correlations with coral cover were not significant, nutrient stoichiometry is best interpreted here as a potential contextual modifier rather than an independent driver of the observed benthic patterns. The enrichment of FA at coral tissue margins at PM and TG is consistent with the possibility that nutrient imbalance may contribute to macroalgal performance at environmentally stressed sites, but that mechanism was not directly tested in the present study (Rasher et al. 2011; Rosset et al. 2017; Lapointe et al. 2019; Adam et al. 2021).

Temperature and salinity variations among sites also potentially modulated competitive dynamics, though their direct effects appeared less pronounced than those of sedimentation. Thermally more stable sites (*e.g.,* AH) supported higher coral cover despite moderate macroalgal presence, while sites experiencing thermal extremes and elevated variability (TG: warmest temperatures; Fig. 1C) exhibited reduced coral abundance, consistent with increased bleaching susceptibility and thermal stress mortality (Spalding and Brown 2015; Jones and Gilliam 2024).

Taken together, the results suggest that competitive outcomes covary with the cumulative stress load of co-occurring environmental factors more than with any isolated stressor effect, consistent with theoretical frameworks that emphasize interacting stressors in driving patterns consistent with benthic state shifts (Hughes 1994; Bellwood et al. 2004).

Macroalgal functional identity, environmental context, and the modulation of competitive vulnerability

Competition for benthic space constitutes a fundamental ecological process structuring coral reef communities, with interaction outcomes directly influencing habitat quality and ecosystem function (Connell et al. 2004; Ferrari et al. 2012; González-Rivero et al. 2016; Horwitz et al. 2017). The results of Sect. "Coral–Macroalgae competitive outcomes are mediated by functional identity and environmental context." showed that macroalgal functional identity exerts a stronger influence on competitive outcomes at the coral–algal interface, exerting a more consistent structuring influence than coral morphology category (Fig. 3C, S3F). These findings are consistent with established ecological theory identifying macroalgal growth form, sediment-trapping capacity, and allelopathic potential as key drivers of coral competitive performance (McCook et al. 2001; Rasher et al. 2011; Liao et al. 2019), and extend these observations across a natural environmental gradient characteristic of Caribbean fringing reefs.

Among the three macroalgal functional groups assessed, FTA won significantly more interactions than both CA ($p < 0.01$) and FA ($p < 0.01$), while CA and FA did not differ from one another ($p > 0.05$; Fig. 3C, S3D). Importantly, FTA competitive superiority outcomes varied significantly among sites and were most distinct at TG and PM (both $p < 0.05$) but were statistically equivalent at PS and AH (all $p > 0.05$; Fig. S3D), suggesting that FTA competitive advantage was most pronounced under elevated sedimentation and associated environmental stress. This site-specific modulation is consistent with prior evidence that FTA growth, sediment retention, and physiological impact on adjacent coral tissue are amplified under turbid, high-nutrient conditions (Goatley and Bellwood 2013; Tebbett et al. 2018). The mechanistic pathways underlying FTA competitive dominance, including rapid substrate colonization, generation of hypoxic microenvironments at coral–macroalgal boundary (Wangpraseurt et al. 2012; Roach et al. 2020), and physical tissue damage, are drawn from prior experimental work and are invoked here as plausible explanations for the observed competitive hierarchy; not directly measured in this study.

Although FA did not emerge as statistically superior in the functional-group analysis (global FA site-level variation: $p = 0.196$; Fig. S3E), FA was significantly more abundant at coral tissue margins at PM and TG relative to background benthic abundance (Fig. 3A), indicating disproportionate contact with coral tissue at the two highest-sedimentation sites. This overrepresentation at degraded sites, despite the absence of a statistically significant outcome advantage, may reflect: (i) elevated FA biomass generating more frequent physical contact independent of competitive prowess; (ii) the allelopathic and lateral-encroachment mechanisms that operate over longer time scales than the snapshot assessments employed here (Rasher and Hay 2010b; Ferrari et al. 2012; Brown et al. 2020); and (iii) sediment-loaded FA thalli may augment competitive capacity under chronically turbid conditions prevailing at TG and PM (Liao et al. 2019). The marginal AH–PS pairwise contrast ($p = 0.042$) falls well above the Bonferroni-adjusted threshold ($p < 0.0083$) and should not be interpreted as evidence of a robust site-level effect.

The significant abundance of CA at coral tissue margins at AH (the site with the lowest sedimentation rate, highest coral cover, and highest *D. antillarum* density; Fig. 3A) provides an ecologically informative complement to FA and FTA patterns. Coralline algae are generally poor competitors under elevated nutrient and sediment loading (Bellwood et al. 2004; Tebbett et al. 2018), and their disproportionate representation at coral margins at AH likely reflects the comparatively benign abiotic conditions at this site. The identity of the macroalgal type encountered at the coral–macroalgal interface is therefore itself an indicator of ambient

environmental quality: Under relatively favorable conditions, competitive interactions are more likely to involve low-impact adversaries (CA), whereas the higher-sedimentation sites are characterized by functionally aggressive FTA and FA. This observation reinforces the context-dependent framing and underscores that competitive dynamics cannot be characterized independently of the environmental matrix in which they occur.

Coral competitive outcomes did not vary significantly among coral morphological categories ($p = 0.381$; Fig. S3F), these non-significant differences may reflect limited statistical power associated with uneven representation among morphology categories. Descriptively, branching *Porites* spp. achieved higher coral wins against FA (Fig. S3F), consistent with "vertical escape" strategies in which upright growth can reduce lateral macroalgae encroachment and improve sediment-shedding capacity (Swierts and Vermeij 2016). By contrast, encrusting and massive morphologies appeared more susceptible to FTA overgrowth, aligning with theoretical predictions that three-dimensional colony architecture can reduce sediment accumulation and confer light-competition advantages (Vermeij et al. 2010; Swierts and Vermeij 2016). Overall, competitive outcomes at coral–macroalgae interface appear hierarchically structured: Macroalgal functional identity represents the primary determinant, environmental context modulates site-specific effects, and coral morphology likely exerts a secondary influence that remained statistically unresolved here. Larger sample sizes are needed to test these patterns robustly for restoration-relevant inference.

Context-dependent herbivory and environmental modulation of benthic-community regulation

Although the broader environmental gradient suggests that the two lower-sedimentation sites (AH and PS) maintained higher coral cover than the two higher-sedimentation sites (PM and TG), this pattern should be interpreted as a site-level association rather than as evidence that sedimentation alone determines herbivore regulatory efficacy. Within-site analyses (Fig. 5B–C; Table S2) did not support a simple dose-dependent top-down suppression model. Coral cover was not significantly predicted by *D. antillarum* density at any site, and where macroalgal cover was significantly associated with urchin density, the association was positive rather than negative. These results indicate that the relationship between herbivore abundance and benthic organization is context dependent and may be shaped by habitat structure, resource distribution, or shared environmental drivers, rather than by a uniform direct grazing effect detectable at the transect scale.

An additional consideration is that the recovery of *D. antillarum* population may depend not only on increases in density but also on habitat structural complexity, larval settlement dynamics, and changes in size structure, as larger individuals generally can exert stronger grazing effects than smaller ones, which may influence benthic-community dynamics (Precht and Precht 2015; Rogers and Lorenzen 2016; Bodmer et al. 2021; Hylkema and Klokman 2025). At AH, the population included more medium and large urchins compared with PS and TG, suggesting that demographic structure may contribute to site-level differences in benthic condition by altering the potential grazing capacity of populations. However, this interpretation remains hypothetical and requires direct measurements of grazing rates and demographic contributions to herbivory.

This pattern, in which higher *D. antillarum* densities coincide with higher rather than lower macroalgal cover, is inconsistent with a straightforward density-dependent grazing-suppression model operating at the transect scale, a comparable pattern is not unprecedented: Sustained macroalgal dominance despite the local presence of recovering *D. antillarum* populations has been reported elsewhere in the Caribbean (Steiner and Williams 2006; Lacey et al. 2013). The cross-sectional, transect-level design employed here cannot distinguish whether sea urchins aggregate in response to existing macroalgal abundance or whether grazing intensity is simply insufficient to overcome macroalgal productivity at the densities observed; both processes are ecologically plausible and not mutually exclusive. However, the macroalgal dominance at the more sediment-impacted sites regardless of herbivore density may suggest that chronic environmental stress can reduce or obscure grazing effects. Although experimental validation is required, these relationships are consistent with prior evidence that elevated sediment and nutrient loading can progressively constrain herbivore-mediated control of macroalgae (Hixon 2015; Sangil and Guzman 2020; Wakwella et al. 2020; Fong et al. 2024).

These within-site results complement, rather than contradict, the negative association between *D. antillarum* density and the probability of macroalgal win identified at the level of individual coral–macroalgal interactions (logistic regression: $\beta = -3.06$, $p = 0.0008$). As previously noted, this relationship most plausibly reflects spatial covariance between herbivore abundance and other favorable site-level conditions, particularly lower sedimentation, rather than a direct, density-dependent grazing effect; this interpretation is now reinforced by the absence of any significant within-site relationship between urchin density and coral cover at the transect scale (Fig. 5B).

Tweedie GLM analyses clarified these site-level patterns of benthic organization (Table S2). At AH the negative coral–macroalgal association (Fig. S5A) is consistent with a scenario in which herbivory may contribute to limiting macroalgal dominance under favorable environmental conditions, paralleling phase-shift reversals following *D.*

antillarum recovery (Lessios 1988, 2016; Knowlton 2001; Carpenter and Edmunds 2006; Idjadi et al. 2010; Levitan et al. 2023). At PS, the significant positive association ($\beta = 2.856$, $p = 0.002$; Fig. S5B) despite the lowest *D. antillarum* density of all sites may more plausibly reflect shared dependence on substrate availability or habitat structure than competitive exclusion or loss-of-grazing control. This reframes PS not as a site where herbivore regulation has failed, but as one where coral–macroalgal organization follows a fundamentally different ecological logic than at AH. At PM and TG, zero-inflated data precluded coherent interpretation, and no regulatory state is inferred. Collectively, these site-specific contrasts suggest that *D. antillarum* influence on benthic composition is contingent on local environmental context, consistent with frameworks wherein bottom-up stressors progressively reshape, rather than simply override, the top-down grazing control (Burkepile and Hay 2006; Tebbett et al. 2018; Munsterman et al. 2021; Tebbett and Bellwood 2021).

Taken together, these analyses indicate that the regulatory influence of *D. antillarum* on benthic composition, if present, operates more plausibly as a coarse-grained, environmentally contingent phenomenon manifesting across the sedimentation gradient between sites than as a fine-grained, transect-level dose–response relationship within a site. This distinction underscores the importance of explicitly considering spatial scale when evaluating herbivore-mediated regulation in heterogeneous reef systems and indicates that broader spatial replication and manipulative experiments capable of decoupling grazer aggregation from grazing impact are required to resolve the mechanistic basis of the patterns reported here.

Co-occurring environmental effects and patterns consistent with ecosystem state transitions

Integration of environmental gradients with biological interactions revealed site-level patterns consistent with cumulative environmental modulation of benthic-community organization. The lower-sedimentation sites retained higher coral cover and more mixed assemblages, whereas the higher-sedimentation sites were characterized by lower coral cover and competitive environments less favorable to coral persistence. These contrasts are compatible with conceptual frameworks of benthic state change (Hughes 1994), but the observational design and limited replication across only four sites do not permit inference about fixed ecological breakpoints or the mechanistic demonstration of persistent alternative states. Instead, the present data support a more cautious interpretation in which co-occurring environmental stressors may progressively reduce the conditions under which herbivory contributes to favorable coral-associated benthic organization. Under comparatively low environmental stress, top-down herbivore control exhibited benthic patterns consistent with lower macroalgal cover and maintenance of coral-dominated assemblages (Bellwood et al. 2004; Hughes et al. 2007). Under elevated environmental stress, bottom-up forcing (*i.e.,* through nutrient enrichment and sediment loading) likely reduces the capacity of grazers to suppress macroalgal proliferation, consistent with experimental and observational evidence from the Caribbean and Indo-Pacific systems (Burkepile and Hay 2006; Tebbett and Bellwood 2021).

Positive feedback mechanisms may further reinforce toward alternative community states once environmental stress reaches levels that constrain herbivore regulatory capacity. Elevated nutrient and sediment inputs favor macroalgal growth and recruitment, which in turn traps additional sediment particles and reduces suitable settlement substrate for corals and *D. antillarum* larvae, potentially creating hysteresis wherein ecosystem recovery requires substantially greater improvements in environmental quality than the level of degradation that facilitated the initial transition (Hughes 1994; Smith et al. 2010; Goatley and Bellwood 2013). As emphasized throughout, the site-level sedimentation contrasts described here should be interpreted as descriptive observations derived from spatial covariation across only four sites, rather than as evidence of a definitive ecological breakpoint or management target that can be generalized to other reef systems. Within this context, the contrasting benthic states observed among sites are consistent with theoretical frameworks proposing that interacting bottom-up and top-down processes jointly influence reef trajectories and the persistence of coral- versus macroalgal-dominated assemblages (Hughes 1994; Bellwood et al. 2004; Burkepile and Hay 2006).

Conclusion and implications for conservation

This study shows that coral–macroalgae interactions are strongly conditioned by environmental context rather than by any single ecological driver. Across the four study sites, benthic organization and competitive outcomes varied consistently along environmental gradients, with sedimentation emerging as the strongest correlate of reduced coral dominance and coral–macroalgal balance. Macroalgal functional identity further influenced interaction outcomes, with FTA showing the greatest competitive success, while FA was disproportionately represented at coral margins at the more stressed sites. Together, these findings indicate that the identity of interacting competitors and the surrounding environmental setting jointly determine the outcome of coral–macroalgal competition.

The role of *D. antillarum* was similarly context dependent. Although higher urchin abundance was associated with coral-favorable interaction patterns among sites,

within-site analyses did not support a simple density-dependent grazing effect. Instead, the results suggest that herbivore influence is contingent upon local environmental conditions and should be interpreted as one component of a broader network of interacting bottom-up and top-down processes, rather than as an independent or universally dominant regulator of benthic state organization.

From a conservation perspective, these findings emphasize that restoration of herbivore populations alone is unlikely to maximize reef recovery where chronic environmental degradation persists. Reducing land-based sediment inputs, while improving overall water quality, should be considered alongside efforts to restore herbivore populations, as complementary rather than as a separate objective. Although the observational four-site design constrains causal inference, the ecological patterns observed here can provide a framework for future manipulative experiments and broader spatial studies aimed at disentangling the interacting roles of environmental remediation and biological restoration in promoting coral reef persistence under increasing environmental change.

Acknowledgements This material is based upon work supported by Puerto Rico Sea Grant under Grant No. NA22OAR4170097 awarded to JE-L. Support was also provided by the UFF-FIU and the Faculty Senate, Summer Research Enhancement Award for JE-L. This work was also supported by the National Science Foundation under Grants HRD-1547798 and HRD-2111661 awarded to Florida International University as part of the Centers of Research Excellence in Science and Technology (CREST) Program. We thank Dr. Alex Mercado-Molina, Dr. Javier Rodriguez-Casariego, Pedro Gomez, Dr. Kelcie Chiquillo, Dr. Juliet Wong, and André Briscoe for their invaluable logistical and fieldwork support. We also would thank to Juan López-Mendoza for his immense laboratory work and picture analysis support. This is contribution number #2180 from the Institute of Environment, at Florida International University.

Author contributions ITL-J and JE-L designed the work. ITL-J and JE-L performed the fieldwork. ITL-J performed the laboratory work. ITL-J and JE-L analyzed the data. ITL-J and JE-L provided funding. ITL-J and JE-L provided supplies. ITL-J wrote the manuscript with input from all contributing authors. All authors contributed to and approved the submitted version of the manuscript.

Funding Puerto Rico Sea Grant College, University of Puerto Rico, NA22OAR4170097, National Science Foundation, HRD-2111661

Data availability Datasets utilized in the study, which characterize environmental conditions, coral–macroalgal interactions, and *Diadema antillarum* density and test size, along with the associated metadata and data analysis R script can be found in the Zenodo repository (https://zenodo.org/records/18250751) https://doi.org/10.5281/zenodo.18250751

Declarations

Conflict of interest The authors declare that they do not have any known conflicts of interest.

References

Abràmoff M, Magalhães PJ, Ram S (2004) Image Processing with ImageJ Biophotonics International 11:36–42

Adam TC, Burkepile DE, Holbrook SJ, Carpenter RC, Claudet J, Loiseau C, Thiault L, Brooks AJ, Washburn L, Schmitt RJ (2021) Running Head: nutrient enrichment on a coral reef Landscape-scale patterns of nutrient enrichment in a coral reef ecosystem: implications for coral to algae phase shifts. Ecol Appl 31:e2227

Barott KL, Rohwer FL (2012) Unseen players shape benthic competition on coral reefs. Trends Microbiol 20:621–628. https://doi.org/10.1016/j.tim.2012.08.004

Barott K, Smith J, Dinsdale E, Hatay M, Sandin S, Rohwer F (2009) Hyperspectral and physiological analyses of coral-algal interactions. PLoS ONE. https://doi.org/10.1371/journal.pone.0008043

Barott KL, Williams GJ, Vermeij MJA, Harris J, Smith JE, Rohwer FL, Sandin SA (2012) Natural history of coral−algae competition across a gradient of human activity in the Line Islands. Mar Ecol Prog Ser 460:1–12. https://doi.org/10.3354/meps09874

Bellwood DR, Hughes TP, Folke C, Nyström M (2004) Confronting the coral reef crisis. Nature 429:827–833. https://doi.org/10.1038/nature02691

Bellwood DR, Hoey AS, Ackerman JL, Depczynski M (2006) Coral bleaching, reef fish community phase shifts and the resilience of coral reefs: BLEACHING IMPACTS ON CORAL REEFS. Glob Chang Biol 12:1587–1594. https://doi.org/10.1111/j.1365-2486.2006.01204.x

Bessell-Browne P, Negri AP, Fisher R, Clode PL, Duckworth A, Jones R (2017) Impacts of turbidity on corals: the relative importance of light limitation and suspended sediments. Mar Pollut Bull 117:161–170. https://doi.org/10.1016/j.marpolbul.2017.01.050

Birrell CL, McCook LJ, Willis BL (2008) Effects of benthic algae on the replenishment of corals and the implications for the resilience of coral reefs. Oceanography and marine biology. CRC Press, pp 31–70. https://doi.org/10.1201/9781420065756-4

Bodmer MDV, Wheeler PM, Anand P, Cameron SE, Hintikka S, Cai W, Borcsok AO, Exton DA (2021) The ecological importance of habitat complexity to the Caribbean coral reef herbivore *Diadema antillarum*: three lines of evidence. Sci Rep 11:9382. https://doi.org/10.1038/s41598-021-87232-9

Brown KT, Bender-Champ D, Kenyon TM, Rémond C, Hoegh-Guldberg O, Dove S (2019) Temporal effects of ocean warming and acidification on coral–algal competition. Coral Reefs 38:297–309. https://doi.org/10.1007/s00338-019-01775-y

Brown KT, Bender-Champ D, Hoegh-Guldberg O, Dove S (2020) Seasonal shifts in the competitive ability of macroalgae

influence the outcomes of coral-algal competition. R Soc Open Sci 7:201797. https://doi.org/10.1098/rsos.201797
Brown KT, Bender-Champ D, Kubicek A, van der Zande R, Achlatis M, Hoegh-Guldberg O, Dove SG (2018) The dynamics of coral-algal interactions in space and time on the southern great barrier reef. Front Mar Sci 5: https://doi.org/10.3389/fmars.2018.00181
Burkepile DE, Hay ME (2006) Herbivore vs. nutrient control of marine primary producers: context-dependent effects. Ecology 87:3128–3139. https://doi.org/10.1890/0012-9658(2006)87[3128:hvncom]2.0.co;2
Burkepile DE, Hay ME (2010) Impact of herbivore identity on algal succession and coral growth on a Caribbean reef. PLoS ONE 5:e8963. https://doi.org/10.1371/journal.pone.0008963
Carpenter RC, Edmunds PJ (2006) Local and regional scale recovery of Diadema promotes recruitment of scleractinian corals: recovery of Diadema. Ecol Lett 9:271–280. https://doi.org/10.1111/j.1461-0248.2005.00866.x
Cetz-Navarro NP, Espinoza-Avalos J, Hernández-Arana HA, Carricart-Ganivet JP (2013) Biological responses of the coral *Montastraea annularis* to the removal of filamentous turf algae. PLoS ONE 8:e54810. https://doi.org/10.1371/journal.pone.0054810
Cetz-Navarro NP, Quan-Young LI, Espinoza-Avalos J (2015) Morphological and community changes of turf algae in competition with corals. Sci Rep 5:12814. https://doi.org/10.1038/srep12814
Clements CS, Rasher D, Hoey A, Bonito V, Hay M (2018) Spatial and temporal limits of coral-macroalgal competition: the negative impacts of macroalgal density, proximity, and history of contact. Mar Ecol Prog Ser 586:11–20. https://doi.org/10.3354/meps12410
Connell JH, Hughes TP, Wallace CC, Tanner JE, Harms KE, Kerr AM (2004) A long-term study of competition and diversity of corals. Ecol Monogr 74:179–210. https://doi.org/10.1890/02-4043
Estrada-Saldívar N, Quiroga-García BA, Pérez-Cervantes E, Rivera-Garibay OO, Alvarez-Filip L (2021) Effects of the stony Coral Tissue Loss Disease outbreak on coral communities and the benthic composition of Cozumel reefs. Front Mar Sci 8:632777. https://doi.org/10.3389/fmars.2021.632777
Fabricius KE (2005) Effects of terrestrial runoff on the ecology of corals and coral reefs: review and synthesis. Mar Pollut Bull 50:125–146. https://doi.org/10.1016/j.marpolbul.2004.11.028
Ferrari R, Gonzalez-Rivero M, Mumby PJ (2012) Size matters in competition between corals and macroalgae. Mar Ecol Prog Ser 467:77–88. https://doi.org/10.3354/meps09953
Fong C, Smith N, Catalan E, Caraveo B, Barber PH, Fong P (2024) Herbivorous sea urchins (Echinometra mathaei) support resilience on overfished and sedimented tropical reefs. Scientific Reports 14:3829. https://doi.org/10.1038/s41598-024-52222-0
Fox J, Weisberg S (2018) An R companion to applied regression. SAGE Publications, Thousand Oaks, CA
Goatley CHR, Bellwood DR (2013) Ecological consequences of sediment on high-energy coral reefs. PLoS ONE 8:e77737. https://doi.org/10.1371/journal.pone.0077737
Gómez Cubillos MC, Sanjuan Muñoz A, Zea SE, Gómez-Cubillos C (2019) Interacciones de corales masivos con céspedes algales y otros organismos en arrecifes del Parque Nacional Natural Tayrona. Bol Invest Mar Cost 48:143–171. https://doi.org/10.25268/bimc.invemar.2019.48.2.770
González-Rivero M, Bozec Y-M, Chollett I, Ferrari R, Schönberg CHL, Mumby PJ (2016) Asymmetric competition prevents the outbreak of an opportunistic species after coral reef degradation. Oecologia 181:161–173. https://doi.org/10.1007/s00442-015-3541-x
Gowan JC, Tootell JS, Carpenter RC (2014) The effects of water flow and sedimentation on interactions between massive *Porites* and algal turf. Coral Reefs 33:651–663. https://doi.org/10.1007/s00338-014-1154-1
Graham NAJ, Jennings S, MacNeil MA, Mouillot D, Wilson SK (2015) Predicting climate-driven regime shifts versus rebound potential in coral reefs. Nature 518:94–97. https://doi.org/10.1038/nature14140
Haas A, Smith J, Thompson M, Deheyn D (2014) Effects of reduced dissolved oxygen concentrations on physiology and fluorescence of hermatypic corals and benthic algae. PeerJ. https://doi.org/10.7717/peerj.235
Harris RJ, Wilson SK, Fulton CJ (2021) Interactive effects of sediments and urchins on the composition and structure of tropical macroalgal assemblages. Mar Biol 168:144. https://doi.org/10.1007/s00227-021-03953-5
Hixon MA (2015) Reef fishes, seaweeds, and corals. Coral reefs in the Anthropocene. Springer Netherlands, Dordrecht, pp 195–215. https://doi.org/10.1007/978-94-017-7249-5_10
Hoegh-Guldberg O, Poloczanska E, Skirving W, Dove S (2017) Coral Reef Ecosystems under Climate Change and Ocean Acidification. Frontiers in Marine Science 4:158. https://doi.org/10.3389/fmars.2017.00158
Horwitz R, Hoogenboom MO, Fine M (2017) Spatial competition dynamics between reef corals under ocean acidification. Sci Rep 7:40288. https://doi.org/10.1038/srep40288
Hughes TP (1994) Catastrophes, phase shifts, and large-scale degradation of a Caribbean coral reef. Science 265:1547–1551. https://doi.org/10.1126/science.265.5178.1547
Hughes TP, Rodrigues MJ, Bellwood DR, Ceccarelli D, Hoegh-Guldberg O, McCook L, Moltschaniwskyj N, Pratchett MS, Steneck RS, Willis B (2007) Phase shifts, herbivory, and the resilience of coral reefs to climate change. Curr Biol 17:360–365. https://doi.org/10.1016/j.cub.2006.12.049
Hughes TP, Barnes ML, Bellwood DR, Cinner JE, Cumming GS, Jackson JBC, Kleypas J, van de Leemput IA, Lough JM, Morrison TH, Palumbi SR, van Nes EH, Scheffer M (2017a) Coral reefs in the Anthropocene. Nature 546:82–90. https://doi.org/10.1038/nature22901
Hughes TP, Kerry JT, Álvarez-Noriega M, Álvarez-Romero JG, Anderson KD, Baird AH, Babcock RC, Beger M, Bellwood DR, Berkelmans R, Bridge TC, Butler IR, Byrne M, Cantin NE, Comeau S, Connolly SR, Cumming GS, Dalton SJ, Diaz-Pulido G, Eakin CM, Figueira WF, Gilmour JP, Harrison HB, Heron SF, Hoey AS, Hobbs J-PA, Hoogenboom MO, Kennedy EV, Kuo C-Y, Lough JM, Lowe RJ, Liu G, McCulloch MT, Malcolm HA, McWilliam MJ, Pandolfi JM, Pears RJ, Pratchett MS, Schoepf V, Simpson T, Skirving WJ, Sommer B, Torda G, Wachenfeld DR, Willis BL, Wilson SK (2017b) Global warming and recurrent mass bleaching of corals. Nature 543:373–377. https://doi.org/10.1038/nature21707
Hughes TP, Baird AH, Morrison TH, Torda G (2023) Principles for coral reef restoration in the anthropocene. One Earth 6:656–665. https://doi.org/10.1016/j.oneear.2023.04.008
Hylkema A, Klokman OJ (2025) Factors constraining natural recovery of *Diadema antillarum* following a mass die-off: a case study near the island of Saba, Caribbean Netherlands. PeerJ 13:e20418. https://doi.org/10.7717/peerj.20418
Idjadi JA, Haring RN, Precht WF (2010) Recovery of the sea urchin *Diadema antillarum* promotes scleractinian coral growth and survivorship on shallow Jamaican reefs. Mar Ecol Prog Ser 403:91–100. https://doi.org/10.3354/meps08463
Jompa J, McCook L (2003) Coral-algal competition: macroalgae with different properties have different effects on corals. Mar Ecol Prog Ser 258:87–95. https://doi.org/10.3354/MEPS258087
Jones NP, Gilliam DS (2024) Temperature and local anthropogenic pressures limit stony coral assemblage viability in southeast Florida. Mar Pollut Bull 200:116098. https://doi.org/10.1016/j.marpolbul.2024.116098
Knowlton N (2001) Sea urchin recovery from mass mortality: new hope for Caribbean coral reefs? Proc Natl Acad Sci U S A 98:4822–4824. https://doi.org/10.1073/pnas.091107198

Kohler KE, Gill SM (2006) Coral point count with Excel extensions (CPCe): a Visual Basic program for the determination of coral and substrate coverage using random point count methodology. Comput Geosci 32:1259–1269. https://doi.org/10.1016/j.cageo.2005.11.009

Kuffner IB, Walters LJ, Becerro MA, Paul VJ, Ritson-Williams R, Beach KS (2006) Inhibition of coral recruitment by macroalgae and cyanobacteria. Mar Ecol Prog Ser 323:107–117. https://doi.org/10.3354/meps323107

Lacey EA, Fourqurean JW, Collado-Vides L (2013) Increased algal dominance despite presence of *Diadema antillarum* populations on a Caribbean coral reef. Bull Mar Sci 89:603–620. https://doi.org/10.5343/bms.2012.1015

Lapointe BE, Brewton RA, Herren LW, Porter JW, Hu C (2019) Nitrogen enrichment, altered stoichiometry, and coral reef decline at Looe Key, Florida Keys, USA: a 3-decade study. Mar Biol 166:108. https://doi.org/10.1007/s00227-019-3538-9

Lesser M (2021) Eutrophication on coral reefs: what is the evidence for phase shifts, nutrient limitation and coral bleaching. Bioscience 71:1216-1233. https://doi.org/10.1093/biosci/biab101

Lessios H (1988) Mass mortality of *Diadema antillarum* in the Caribbean: what have we learned? Annu Rev Ecol Evol Syst 19:371–393. https://doi.org/10.1146/ANNUREV.ES.19.110188.002103

Lessios HA (2016) The great *Diadema antillarum* die-off: 30 years later. Ann Rev Mar Sci 8:267–283. https://doi.org/10.1146/annurev-marine-122414-033857

Levitan DR, Best RM, Edmunds PJ (2023) Sea urchin mass mortalities 40 y apart further threaten Caribbean coral reefs. Proc Natl Acad Sci U S A 120:e2218901120. https://doi.org/10.1073/pnas.2218901120

Liao Z, Yu K, Wang Y, Huang X, Xu L (2019) Coral-algal interactions at Weizhou Island in the northern South China Sea: variations by taxa and the exacerbating impact of sediments trapped in turf algae. PeerJ 7:e6590. https://doi.org/10.7717/peerj.6590

Littler MM, Littler DS (2007) Assessment of coral reefs using herbivory/nutrient assays and indicator groups of benthic primary producers: a critical synthesis, proposed protocols, and critique of management strategies. Aquat Conserv 17:195–215. https://doi.org/10.1002/aqc.790

Littler MM, Littler DS, Brooks BL (2009) Herbivory, nutrients, stochastic events, and relative dominances of benthic indicator groups on coral reefs: a review and recommendations. Smithson Contrib Mar Sci 38:401–414

López-Jiménez IT, Quan-Young LI, Florez-Leiva L (2021) Effect of terrigenous sediments on macroalgae functional-form groups of coral reefs in Capurganá, Colombian Caribbean. Sci Mar 85:125–135. https://doi.org/10.3989/scimar.05146.013

McCook L, Jompa J, Diaz-Pulido G (2001) Competition between corals and algae on coral reefs: a review of evidence and mechanisms. Coral Reefs 19:400–417. https://doi.org/10.1007/s003380000129

Mercado-Molina AE, Montañez-Acuña A, Rodríguez-Barreras R, Colón-Miranda R, Díaz-Ortega G, Martínez-González N, Schleier-Hernández S, Sabat AM (2015) Revisiting the population status of the sea urchin *Diadema antillarum* in northern Puerto Rico. J Mar Biol Assoc U K 95:1017–1024. https://doi.org/10.1017/s002531541400188x

Munsterman KS, Allgeier JE, Peters JR, Burkepile DE (2021) A view from both ends: shifts in herbivore assemblages impact top-down and bottom-up processes on coral reefs. Ecosystems (n y) 24:1702–1715. https://doi.org/10.1007/s10021-021-00612-0

Otaño-Cruz A, Montañez-Acuña AA, Torres-López V, Hernández-Figueroa EM, Hernández-Delgado EA (2017) Effects of changing weather, oceanographic conditions, and land uses on spatio-temporal variation of sedimentation dynamics along near-shore coral reefs. Front Mar Sci 4:249. https://doi.org/10.3389/fmars.2017.00249

Pozas-Schacre C, Bischoff H, Clerissi C, Nugues MM (2024) Negative parental and offspring environmental effects of macroalgae on coral recruitment are linked with alterations in the coral larval microbiome. R Soc Open Sci 11:240187. https://doi.org/10.1098/rsos.240187

Precht LL, Precht W (2015) The sea urchin Diadema antillarum – keystone herbivore or redundant species? PeerJ PrePrints. https://doi.org/10.7287/PEERJ.PREPRINTS.1565V2

Preskitt LB, Vroom PS, Smith CM (2004) A rapid ecological assessment (REA) quantitative survey method for benthic algae using photoquadrats with scuba. Pac Sci 58:201–209. https://doi.org/10.1353/psc.2004.0021

Rasher DB, Hay ME (2010a) Seaweed allelopathy degrades the resilience and function of coral reefs. Commun Integr Biol 3:564–566. https://doi.org/10.4161/cib.3.6.12978

Rasher DB, Hay ME (2010b) Chemically rich seaweeds poison corals when not controlled by herbivores. Proc Natl Acad Sci U S A 107:9683–9688. https://doi.org/10.1073/pnas.0912095107

Rasher D, Stout EP, Engel S, Kubanek J, Hay M (2011) Macroalgal terpenes function as allelopathic agents against reef corals. Proc Natl Acad Sci U S A 108:17726–17731. https://doi.org/10.1073/pnas.1108628108

Redfield AC (1958) The biological control of chemical factors in the environment. Am Sci

Roach TNF, Little M, Arts MGI, Huckeba J, Haas AF, George EE, Quinn RA, Cobián-Güemes AG, Naliboff DS, Silveira CB, Vermeij MJA, Kelly LW, Dorrestein PC, Rohwer F (2020) A multiomic analysis of in situ coral-turf algal interactions. Proc Natl Acad Sci U S A 117:13588–13595. https://doi.org/10.1073/pnas.1915455117

Rodríguez-Barreras R, Dominicci-Maura A, Tosado-Rodríguez EL, Godoy-Vitorino F (2023) The epibiotic microbiota of wild Caribbean sea urchin spines is species specific. Microorganisms 2:391. https://doi.org/10.3390/microorganisms11020391

Rogers A, Lorenzen K (2016) Does slow and variable recovery of Diadema antillarum on Caribbean fore-reefs reflect density-dependent habitat selection? Front Mar Sci 3:63. https://doi.org/10.3389/fmars.2016.00063

Rosset S, Wiedenmann J, Reed AJ, D'Angelo C (2017) Phosphate deficiency promotes coral bleaching and is reflected by the ultrastructure of symbiotic dinoflagellates. Mar Pollut Bull 118:180–187. https://doi.org/10.1016/j.marpolbul.2017.02.044

Sangil C, Guzman HM (2020) Macroalgal community response to herbivores and sediment deposition: an indicator of coral reef degradation. J Appl Phycol 32:1405–1419. https://doi.org/10.1007/s10811-019-01991-7

Shantz AA, Ladd MC, Schrack E, Burkepile DE (2015) Fish-derived nutrient hotspots shape coral reef benthic communities. Ecol Appl 25:2142–2152. https://doi.org/10.1890/14-2209.1

Skowronski JS, Sharp WC, Spiers LJ, Feehan CJ (2025) Spatiotemporal patterns in *Diadema antillarum* settlement in the Florida Keys: implications for habitat restoration. Coral Reefs 44:911–922. https://doi.org/10.1007/s00338-025-02656-3

Smith JE, Hunter CL, Smith CM (2010) The effects of top-down versus bottom-up control on benthic coral reef community structure. Oecologia 163:497–507. https://doi.org/10.1007/s00442-009-1546-z

Spalding MD, Brown BE (2015) Warm-water coral reefs and climate change. Science 350:769–771. https://doi.org/10.1126/science.aad0349

Steiner SCC, Williams SM (2006) The density and size distribution of *Diadema antillarum* in Dominica (Lesser Antilles): 2001–2004. Mar Biol 149:1071–1078. https://doi.org/10.1007/s00227-006-0279-3

Swierts T, Vermeij MJ (2016) Competitive interactions between corals and turf algae depend on coral colony form. PeerJ 4:e1984. https://doi.org/10.7717/peerj.1984

Tebbett SB, Bellwood DR (2021) Algal turf productivity on coral reefs: a meta-analysis. Mar Environ Res 168:105311. https://doi.org/10.1016/j.marenvres.2021.105311

Tebbett SB, Bellwood DR, Purcell SW (2018) Sediment addition drives declines in algal turf yield to herbivorous coral reef fishes: implications for reefs and reef fisheries. Coral Reefs 37:929–937. https://doi.org/10.1007/s00338-018-1718-6

Tebbett SB, Crisp SK, Evans RD, Fulton CJ, Pessarrodona A, Wernberg T, Wilson SK, Bellwood DR (2023) On the challenges of identifying benthic dominance on Anthropocene coral reefs. Bioscience 73:220–228. https://doi.org/10.1093/biosci/biad008

Thinesh T, Jose PA, Ramasamy P, Meenatchi R, Selvan K, Selvin J (2019) Differential coral response to algae contact: *Porites* tissue loss, praise for *Halimeda* interaction at southeast coast of India. Environ Sci Pollut Res 26:17845–17852. https://doi.org/10.1007/s11356-019-05024-1

Todd B, Ballantine DL, Otero E (2009) Nutrient distribution across the insular shelf of La Parguera, Puerto Rico: assessment by algal tissue nitrogen. Caribb J Sci 45:181–190. https://doi.org/10.18475/cjos.v45i2.a6

Vermeij MJA, Smith JE, Smith CM, Vega Thurber R, Sandin SA (2009) Survival and settlement success of coral planulae: independent and synergistic effects of macroalgae and microbes. Oecologia 159:325–336. https://doi.org/10.1007/s00442-008-1223-7

Vermeij MJA, van Moorselaar I, Engelhard S, Hörnlein C, Vonk SM, Visser PM (2010) The effects of nutrient enrichment and herbivore abundance on the ability of turf algae to overgrow coral in the Caribbean. PLoS ONE 5:e14312. https://doi.org/10.1371/journal.pone.0014312

Wakwella A, Mumby PJ, Roff G (2020) Sedimentation and overfishing drive changes in early succession and coral recruitment. Proc Biol Sci 287:20202575. https://doi.org/10.1098/rspb.2020.2575

Wangpraseurt D, Weber M, Røy H, Polerecky L, de Beer D, Suharsono NMM (2012) In situ oxygen dynamics in coral-algal interactions. PLoS ONE 7:e31192. https://doi.org/10.1371/journal.pone.0031192

Williams SM (2022) The reduction of harmful algae on Caribbean coral reefs through the reintroduction of a keystone herbivore, the long-spined sea urchin *Diadema antillarum*. Restor Ecol 30:e13475. https://doi.org/10.1111/rec.13475Digital Object Identifier (DOI)